Available online at www.sciencedirect.com

SciVerse ScienceDirect

Ceramics International 39 (2013) 7077–7087

CERAMICS INTERNATIONAL

www.elsevier.com/locate/ceramint

Effect of micro- and nano-fillers on the properties of silicone rubber-alumina flexible microwave substrate

L.K. Namitha, J. Chameswary, S. Ananthakumar, M.T. Sebastian*

Materials Science & Technology Division, National Institute for Interdisciplinary Science & Technology, Trivandrum 695019, India

Received 10 January 2013; received in revised form 15 February 2013; accepted 15 February 2013
Available online 26 February 2013

Abstract

Silicone rubber composites filled with micro- and nano-alumina were prepared and the effect of filler contents on the microwave dielectric, mechanical, thermal and moisture absorption properties were investigated. The composite with 0.45 volume fraction (V_f) of micro alumina has a relative permittivity (ε_r) of 5.89 and dielectric loss (tan δ) of 9×10^{-3} whereas 0.05 volume fraction of nano-alumina has ε_r of 3.52 and tan δ of 1.97×10^{-2}, respectively at 5 GHz. The experimental ε_r and tan δ values of silicone rubber-micro-alumina composites were compared with that of theoretical models. Among the theoretical models Modified Lichtenecker and Parallel model are in good agreement with experimental values of ε_r and tan δ respectively. The silicone rubber nano-alumina composites have better mechanical properties. The coefficient of thermal expansion (CTE) of composites decreased and the moisture absorption increased with increasing amount of filler loading. The improved properties indicate that the silicone rubber-micro-alumina composite is a good candidate for a flexible microwave substrate application.

Keywords: A. Hot pressing; B. Composites; C. Dielectric properties; D. Al_2O_3; E. Substrates

1. Introduction

Microelectronic packaging has been playing a key role in the rapid development of the electronic technologies. Flexible electronics creates a new era in the fast growing electronic industry. Flexible electronics are increasingly being used which benefits from their mechanical flexibility, light weight and favorable dielectric properties [1]. Flexible and stretchable electronics enable a wide range of applications such as capacitors for energy storage, microwave absorbers, flexible dielectric wave guide, flexible displays, sensor arrays, curved circuits, flexible antenna, etc. [2,3]. Recent years have witnessed an expanding interest in the application of flexible polymer materials (e.g., polyimide, polystyrene, polyethylene, etc.) as the substrates for electronic and display devices [4].

The requirements for an ideal microwave substrate material are low dielectric loss for better performance, low relative permittivity to increase signal propagation speed, good flexibility, high thermal conductivity and low coefficient of thermal expansion [5–8]. Several ceramics have the desired dielectric properties but the high processing temperature and brittle nature greatly limits their practical use. The polymer materials meet the requirements like mechanical flexibility, light weight, enhanced durability, ease of processing, low cost, etc. [9]. However, their high coefficient of thermal expansion and low thermal conductivity limit their practical applications [10]. The individual properties of both polymers and ceramics can be tailored through composite approach where they provide useful properties for microwave substrate and electronic packaging applications. The objective of the present study is to develop flexible microwave substrate for electronic applications.

Among the available elastomers, silicone rubber was chosen as rubber matrix. The most outstanding property of silicone rubber is its excellent dielectric properties including low relative permittivity, low dielectric loss (ε_r=3-3.5, tan $\delta = 10^{-3}$ at 1 MHz) and high stretchability [11,12]. Besides dimethyl silicone rubber has highly elastic,

*Corresponding author. Tel.: +91 471 251 5294; fax: +91 471 249 1712.
E-mail address: mailadils@yahoo.com (M.T. Sebastian).

0272-8842/$ - see front matter © 2013 Elsevier Ltd and Techna Group S.r.l. All rights reserved.
http://dx.doi.org/10.1016/j.ceramint.2013.02.047

non-flammable, water and chemical resistant characteristics. The high binding energy of the silicon–oxygen bond (445 kJ/mol) makes them chemically stable even at high temperatures up to 300 °C. The ceramic used in the present study was alumina which is having good dielectric properties ($\varepsilon_r = 9.7-10.5$, tan $\delta = 2\times10^{-4}$ at1 MHz), low CTE, high thermal conductivity and low cost. etc. [6,13].

Extensive work has been done on ceramic filled polymers for electronic packaging and microwave absorption applications [14,15]. Considerable amount of work has been reported on silicone rubber–ceramic composites. However, very little attention was paid on the microwave dielectric properties, Volakis and co-workers studied the ceramic ($BaTiO_3$, Mg–Ca–Ti and Bi–Ba–Nd–Titanate) reinforced polydimethyl siloxane (PDMS) composite substrates for conformal microwave applications in the frequency range, 100 MHz–20 GHz [12]. The dispersion of ferroelectric ceramic powder of lead magnesium niobate–lead titanate (PMN–PT) into silicone rubber matrix and the improvement of dielectric, mechanical and electrical properties was investigated by Gallone et al. [16]. Dielectric properties of calcium copper titanate–silicone resin composites were reported by Babu et al. [17]. Liou and Chiou reported the dielectric tunability of barium strontium titanate–silicone rubber composites for various filler volume fraction [18]. Recently Sim et al. examined the thermal properties of silicone rubber filled with thermally conductive, electrically insulating Al_2O_3, AlN and ZnO for elastomeric thermal pads [19]. The effects of thermally conductive filler type, volume fraction of the filler and filler particle size distribution on the thermal conductivity and viscosity of room-temperature-vulcanized (RTV) silicone rubber was investigated by Wang and Xie [20]. Zhou et al. and Wen-ying et al. investigated the effect of alumina particle size on the mechanical, thermal and physical properties of alumina reinforced silicone rubber composite [11,21]. Recently the microwave dielectric properties of butyl rubber–ceramic composites were investigated by Sebastian and co-workers [22,23]. In this paper we report the effect of micro- and nano-alumina particles on dielectric, mechanical, thermal and moisture absorption properties of silicone rubber composites.

2. Experimental

2.1. Materials and composite preparations

The rubber used was methyl end blocked silicone rubber (molecular weight = 4, 27,000 g/mol) provided by Jyothi rubbers, Thrissur, India. Dicumyl peroxide (DCP) was used as curing agent. Alumina (< 10 μm) and nano-alumina (< 50 nm) were obtained from Sigma Aldrich, USA. The alumina powders were heat treated at 100 °C for 24 h to remove the volatile impurities. The silicone rubber, DCP and ceramic were mixed thoroughly in a kneading machine (Plastomek, Quilandy) with the rotation speed of 25 rpm for 45 min. The kneading machine consists of variable speed mixer having two counter rotating sigma blades. The uniformly mixed composites were hot pressed at 200 °C for 90 min. The optimization of temperature and duration were done by studying the cross linking behavior. The compositions of micro-alumina filled silicone rubber are SRN, SR-mAL_1, SR-mAL_2, SR-mAL_3, SR-mAL_4, SR-mAL_5, SR-mAL_6, SR-mAL_7 and SR-mAL_8 are given in Table 1. The formulations of nano-alumina silicone rubber composites are SR-nAL_1, SR-nAL_2, SR-nAL_3 and SR-nAL_4 are given in Table 2. Maximum filler loading of about $0.45V_f$ is attained for SR-mAL composites while only up to a volume fraction of 0.05 is possible for SR-nAL composites. The mixing became more difficult at higher loadings. For nano-alumina a relatively lower volume fraction (0.05) can only be added to the silicone rubber due to the high surface area of the nano-fillers.

2.2. Characterizations

The swelling test of the rubber was conducted in toluene. The samples were accurately weighed and immersed in a beaker containing toluene for 24 h. These were removed periodically from the bottles and blotted with filter paper to remove excess solvent on the surface and again weighed and then immersed in to the toluene again. The weight swelling ratios (Q) were calculated from the weight of the sample in the unswollen and swollen state using the expression [24]:

$$Q = (M_t - M_0)/M_0 \times 100 \quad (1)$$

Table 2
Formulations of silicone rubber nano-alumina composite.

Ingredients in phr[a]	SRN	SR-nAL_1	SR-nAL_2	SR-nAL_3	SR-nAL_4
Silicone rubber	100	100	100	100	100
Dicumyl peroxide	2	22	2	2	2
Nano-alumina	[b]0 [0]	5 [0.01]	10 [0.02]	15 [0.04]	20 [0.05]

[a]Parts per hundred of rubber.
[b]Volume fractions of filler given in parenthesis.

Table 1
Formulations of silicone rubber micro-alumina composite.

Ingredients in phr[a]	SRN	SR-mAL_1	SR-mAL_2	SR-mAL_3	SR-mAL_4	SR-mAL_5	SR-mAL_6	SR-mAL_7	SR-mAL_8
Silicone rubber	100	100	100	100	100	100	100	100	100
Dicumyl peroxide	2	2	2	2	2	2	2	2	2
Micro alumina	[b]0 [0]	5 [0.01]	10 [0.02]	15 [0.04]	20 [0.05]	50 [0.12]	100 [0.22]	200 [0.35]	300 [0.45]

[a]Parts per hundred of rubber.
[b]Volume fractions of filler given in parenthesis.

where Q is the weight swelling ratio, M_t is the weight of the sample in the swollen state and M_0 is the initial weight of the samples. The samples used for studying the swelling behavior of the peroxide cured silicone rubber have diameter 11 mm and thickness 2 mm. The microstructures of the composites were examined using a scanning electron microscope (SEM) (Jeol Model, JSM 5600LV). Tensile tests on SR-mAL and SR-nAL composites were conducted using dumb-bell shaped samples of width ≈ 4 mm and thickness in the range 2–3 mm. The tensile measurements were carried out in Universal Testing Machine (Hounsfield Model, H5K-S UTM) with a rate of grip separation of 500 mm/min. The frequency dependence of dielectric properties of both SR-mAL and SR-nAL composites were measured at 1 MHz. The variations in the relative permittivity of both SR-mAL and SR-nAL composites with temperature were studied in the temperature range between 25 °C and 80 °C at 1 MHz. The radio frequency dielectric properties were measured by LCR meter (Hioki 3532-50). Thin pellets with diameter 11 mm and thickness < 2 mm were electroded with silver paste on both sides in the form of ceramic capacitors and were used for LCR measurement. Dielectric sheets of dimensions 30 mm × 30 mm and thickness of about 1.8 mm were used for the microwave measurements. The microwave dielectric properties were measured using a Split Post Dielectric Resonator (SPDR) resonating at 5.15 GHz with the help of a Vector network analyzer (Agilent Model, E5071C). The moisture absorption characteristics of the composites were also measured. The samples with dimensions 50 mm × 50 mm × 2 mm were weighed accurately and placed in distilled water for 24 h. The samples were removed, wiped to remove the excess water from the surface and again weighed. The amount of water absorbed was found based on the weight gain of the sample. The volume % of water absorption was calculated using the relation:

$$\text{Volume \% of moisture absorption} = \frac{(W_f - W_i)/\rho_w}{((W_f - W_i)/\rho_w) + (W_i/\rho_c)} \times 100 \quad (2)$$

where W_f and W_i are the final and initial weights of the sample and ρ_w and ρ_c are the densities of water and composite, respectively. The density of the composites was measured using Archimedes method. Coefficient of thermal expansion (CTE) measurements were performed by dilatometer (Netzsch Model, DIL 402 PC) in the temperature range between 25 °C and 150 °C, at a heating rate of 2 °C/min. CTE was determined from the slope of thermal expansion versus temperature plots.

3. Results and discussion

3.1. Swelling behavior

The sorption–desorption method was used to determine the swelling behavior of the vulcanizates [25]. The sorption behavior curve of peroxide cured silicone rubber is shown in Fig. 1. Generally the rate of solvent uptake of elastomer decreased with effective cross linking. The contact of rubber with organic solvent can be well explained by absorption and diffusion phenomena. The diffusion mechanism in rubber is essentially connected with the ability of the polymer to provide pathways for the solvent to progress in the form of randomly generated voids. As the void formation decreases with peroxide curing the solvent uptake also decreases. From the figure it is clear that solvent uptake is lowest for the rubber vulcanized at 200 °C/90 min. It is also evident from the figure that the reinforcement is most effective for the rubber cured at 200 °C/90 min. Hence 200 °C/90 min is taken as the optimized hot pressing condition.

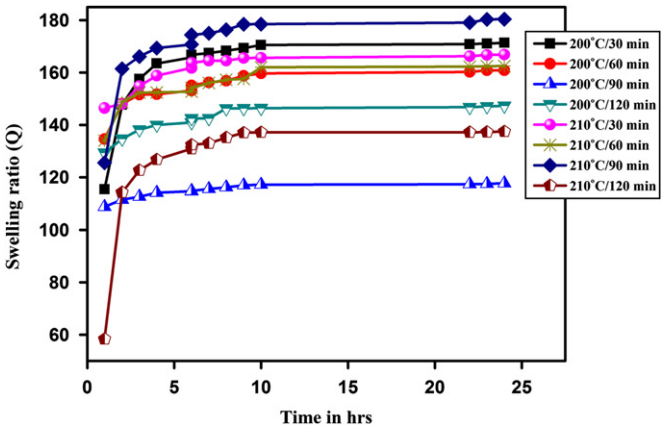

Fig. 1. Swelling ratio as a function of time for peroxide cured silicone rubber at different temperatures.

3.2. Microstructure analysis of the filler and composites

Fig. 2(a) shows the SEM image of micro-alumina particles. From the figure it is clear that the particles are irregularly shaped with average size less than 10 μm. Fig. 2(b)–(i) shows the fractured surface SEM images of SR-mAL composites with different filler loading. It is observed from the figure that the micro-alumina particles are uniformly dispersed throughout the matrix. At lower filler loading the matrix covers the ceramic particles but as the filler loading increases the inter particle distance decreases and this may leads to the agglomeration of filler particles. Porosity is also found to increase with increase in filler loading.

Fig. 3(a) and (b) shows the SEM images of nano-alumina at different magnifications. The fractured surface SEM images of SR-nAL composites are shown in Fig. 3(c)–(f). From the figures it can be inferred that the nano-alumina particles are almost uniformly distributed throughout the matrix. However, nano-alumina particle shows agglomerations at higher filler loading as evidenced by Fig. 3(f).

3.3. Density measurement of the composites

Fig. 4 shows the variations of experimental density of composites with volume fraction of filler. The density of

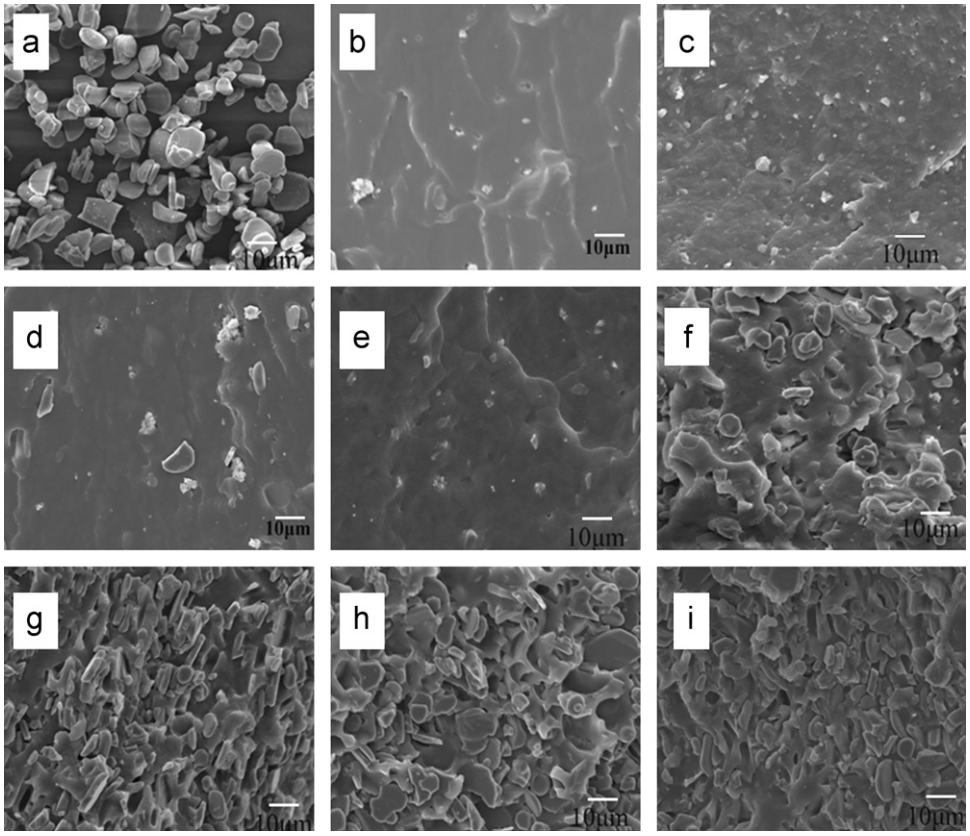

Fig. 2. SEM images of (a) micro-alumina (b–i) cross sectional images of SR-mAL$_1$, SR-mAL$_2$, SR-mAL$_3$, SR-mAL$_4$, SR-mAL$_5$, SR-mAL$_6$, SR-mAL$_7$ and SR-mAL$_8$.

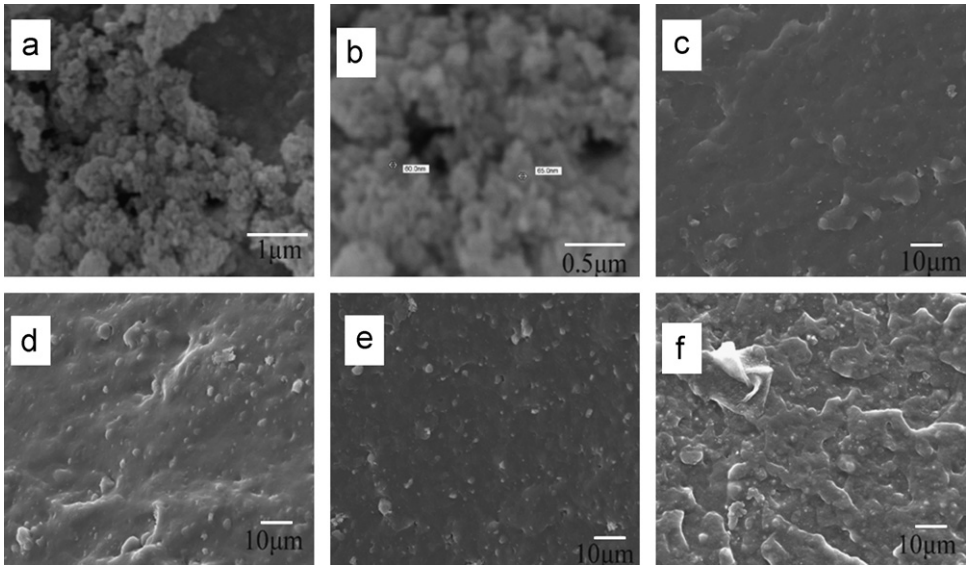

Fig. 3. (a and b) high resolution SEM images of nano-alumina (c–f) cross-sectional surface images of SR-nAL$_1$, SR-nAL$_2$, SR-nAL$_3$ and SR-nAL$_4$ composites.

silicone rubber and composites were measured by Archimedes method. From the figure it is clear that the density of composites increases linearly with increase in the filler content.

3.4. Mechanical properties of the composites

Flexibility is an important property for a substrate material in order to sustain the flexural loading during

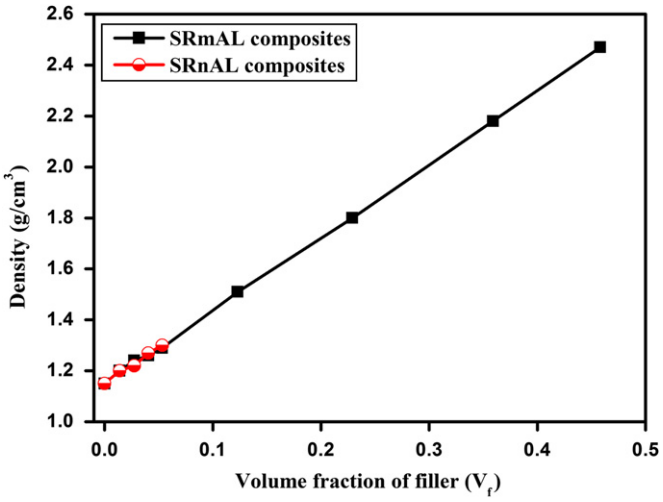

Fig. 4. Variation of experimental density of (a) SR-mAL and (b) SR-nAL composites with filler loading.

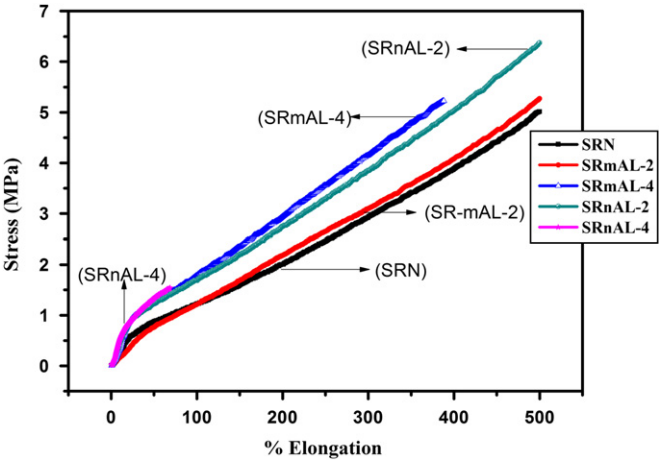

Fig. 5. Stress–strain graph of SR-mAL and SR-nAL composites.

service. Poor flexural rigidity of substrate usually results in excessive warpage and delamination [26]. The mechanical properties of the composites are strongly influenced by the size and shape of the filler, matrix properties as well as the interfacial adhesion between the filler and matrix. The addition of the filler increases the flexural strength of the silicone rubber [27]. Fig. 5 shows the stress–strain curves of SRN, SR-mAL$_2$, SR-mAL$_4$, SR-nAL$_2$ and SR-nAL$_4$. The mechanical strength of the matrix is improved if the particles are well dispersed throughout the composites. The inclusion of finer particles into rubber produces better mechanical properties as compared with larger particles [28]. It is clear from the figure that the nano-alumina filled silicone rubber composites show better reinforcement than the corresponding silicone rubber-micro-alumina composites. As the filler loading increases the flexibility of the composite decreases. It is found that the silicone rubber filled with 20 phr nano-alumina broken at an elongation of 85%. This may be due to the formation of agglomerations at higher ceramic loading which act as weak points in the composite and it easily break when stress is applied [29].

3.5. Dielectric properties of the composites at radio and microwave frequencies.

Fig. 6(a) and (b) shows the variation of relative permittivity with frequency in the range of 1 kHz–3 MHz for SR-mAL and SR-nAL composites. The relative permittivity of SR-mAL composites does not vary much with increase in frequency but the variation is significant for the SR-nAL composites. The relative permittivity shows a dip at a frequency of about 177 kHz due to relaxation at this frequency. The dip gradually disappears with increase in filler content. The plot also shows that the relative permittivity increases as filler content increases. Fig. 7(a) and (b) shows the variation of dielectric loss with log frequency for SR-mAL and SR-nAL composites at 1 kHz–3 MHz. In general, the dielectric loss decreases with increase in frequency. However, the dielectric loss shows an increase at frequencies of about 1.7 kHz and 316 kHz, respectively, due to relaxation. As the ceramic content increases dielectric loss of microcomposites decreases and for nanocomposite it increases. It is known that both relative permittivity and dielectric loss depend on electronic, ionic, dipole-orientation, and space charge polarizations [30]. The present system of

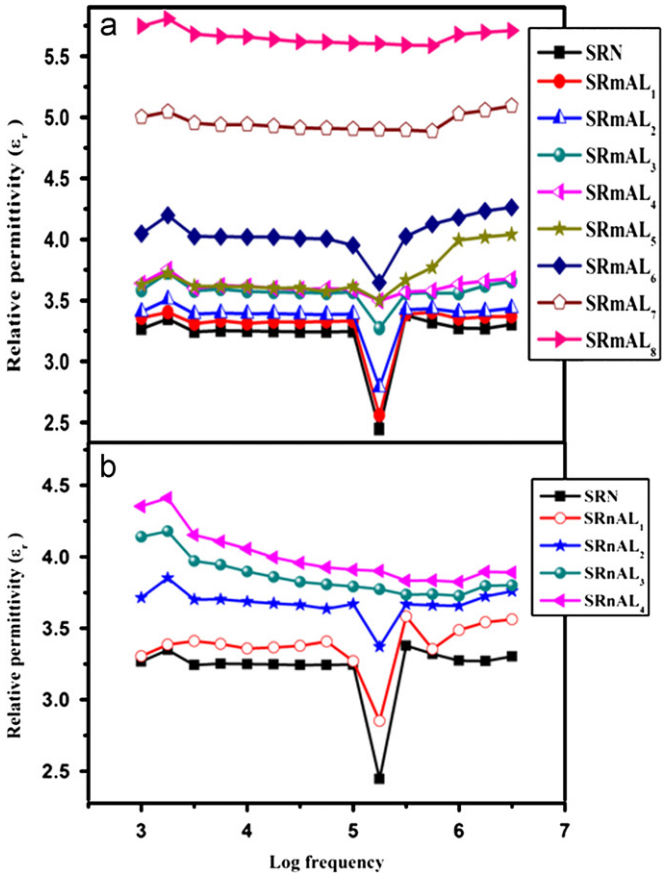

Fig. 6. Variation of relative permittivity with log frequency of (a) SR-mAL composites and (b) SR-nAL composites at 1 MHz.

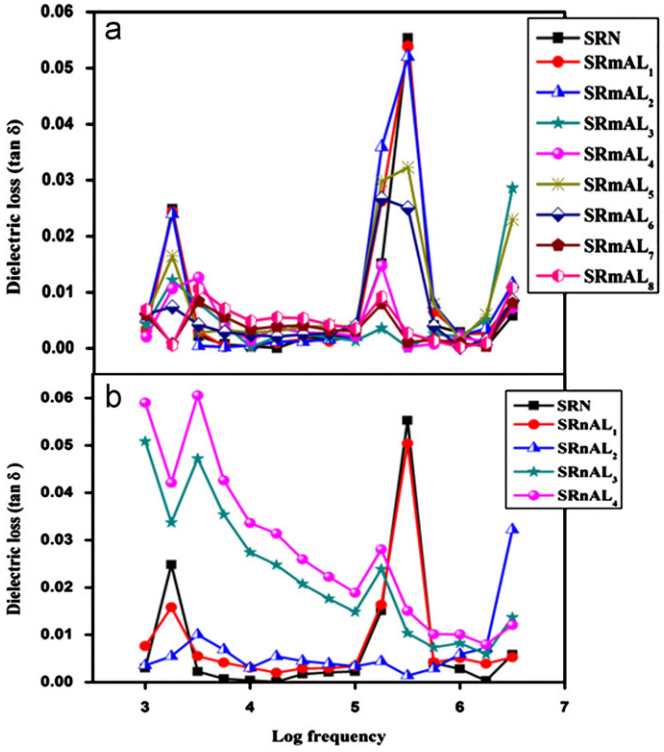

Fig. 7. Variation of dielectric los with log frequency of (a) SR-mAL composites and (b) SR-nAL composites at 1 MHz.

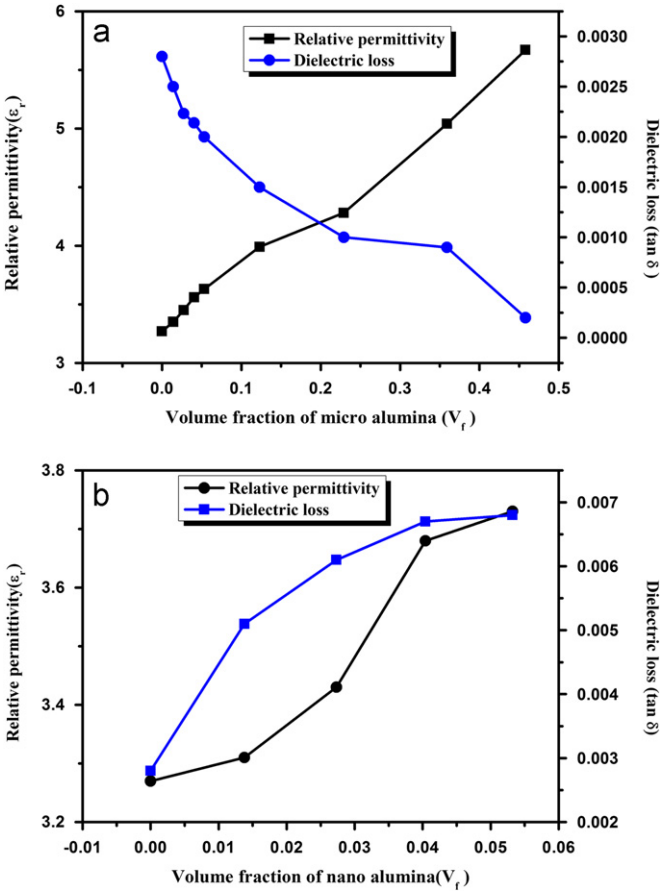

Fig. 8. (a) Variation of relative permittivity and loss tangent of SR-mAL composites at 1 MHz and (b) variation of relative permittivity and loss tangent of SR-nAL composites at 1 MHz.

composite is a biphase mixture of two dielectrically and chemically different materials. Hence the dielectric properties of composites can be affected by the different volume fractions of the fillers and polymer matrix.

A low relative permittivity is desirable for microelectronic packaging to increase the signal transmission speed. The relative permittivity of composites varies between the relative permittivity of polymer and filler. Fig. 8(a) shows the relative permittivity and dielectric loss of SR-mAL composite at 1 MHz. From the figure it is clear that ε_r increases and tan δ decreases with increasing filler content. The dielectric response of the composite at lower filler loading is mainly due to the silicon rubber matrix (SRN have ε_r of 3–3.5 at 1 MHz) and the gradual increase in the relative permittivity of composite with filler content is due to the relatively high relative permittivity of alumina (9.7–10.5 at 1 MHz). At 1 MHz, the relative permittivity of SR-mAL increases from 3.27 to 5.69 with increase in filler loading from 0 to $0.45V_f$. As the filler loading increases the connectivity between filler particles and dipole–dipole interaction increases, which can also lead to an increase in the relative permittivity [31]. Dielectric loss decreases as the volume fraction of micro-alumina increases. This is mainly due to the low loss of alumina filler (2×10^{-4} at 1 MHz) compared to silicone rubber matrix ($\sim10^{-3}$ at 1 MHz). As the filler loading increases from 0–$0.45V_f$, the dielectric loss of SR-mAL composite varies from 2.8×10^{-3} to 2×10^{-4}. Fig. 8(b) depicts the relative permittivity and dielectric loss of SR-nAL composites at 1 MHz. For SR-nAL composites both the relative permittivity and loss factor increases with filler loading. The mixing became more difficult at higher loadings because of the high surface area and larger ceramic volume of nano-fillers which is in agreement with the report of Hu et al. [32]. Maximum filler loading of about $0.45V_f$ is attained for SR-mAL composites while only up to a volume fraction of 0.05 is possible for SR-nAL composites. Zhou et al. reported that after certain volume percentage (40 vol%) of filler loading, hardening and difficulty in processing occurs with degraded mechanical property [28]. At 1 MHz, $0.05V_f$ of filler loading SR-nAL composite has a relative permittivity of 3.73 and dielectric loss of 6×10^{-3}. For the same V_f, SR-mAL composite has relative permittivity and dielectric loss of 3.63 and 2×10^{-3}, respectively. The main drawback of nano-fillers is that the nanoparticles agglomerate easily because of their high surface energy. The main reason for the higher relative permittivity and dielectric loss of nanocomposite is due to its hydrophilic nature.

The variation of microwave dielectric properties of SR-mAL and SR-nAL composites at 5 GHz is shown in Fig. 9(a) and (b), respectively. The microwave dielectric properties have similar behavior as that of radio wave frequencies. The dielectric properties of the composites depend on the loading level of the filler, size and shape of the filler particles and the interfacial properties of the

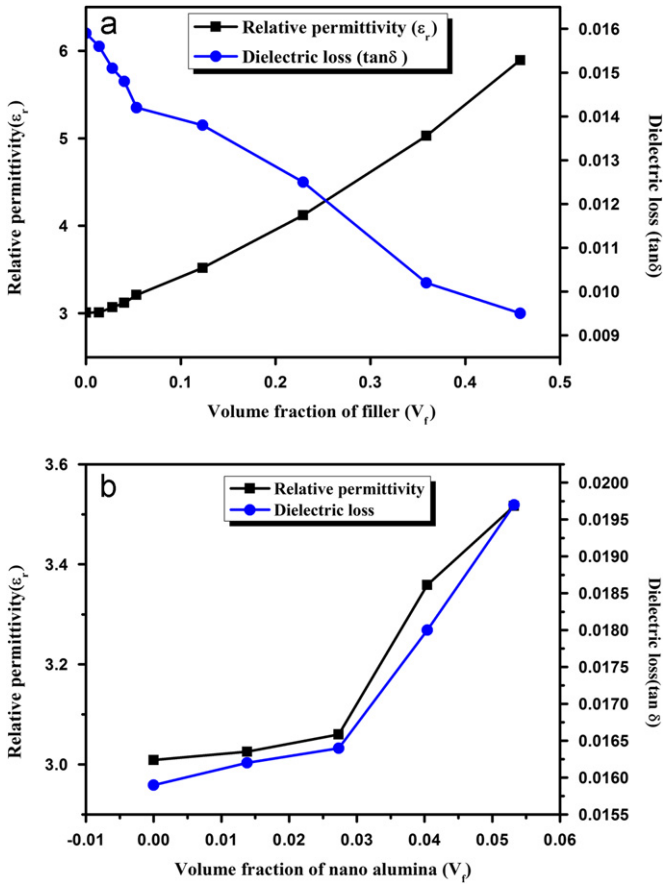

Fig. 9. (a) Variation of relative permittivity and loss tangent of SR-mAL composites at 5 GHz and (b) variation of relative permittivity and loss tangent of SR-nAL composites at 5 GHz.

composites [33]. Fig. 9(a) depicts the relative permittivity and dielectric loss of SR-mAL composites at 5 GHz. The composite has a relative permittivity of 5.89 and a loss tangent of 9×10^{-3} for $0.45V_f$ of SR-mAL composite at 5 GHz. The decrease of effective dielectric loss of composite with increase in filler content is due to the lower dielectric loss of alumina filler (4.3×10^{-5} at 5 GHz) than silicone rubber matrix (1.59×10^{-2} at 5 GHz). Fig. 9(b) shows the relative permittivity and dielectric loss of SR-nAL composite at 5 GHz. The 0.05 volume fraction of micro-alumina loaded silicone rubber composite has a relative permittivity of 3.21 and dielectric loss of 1.42×10^{-2} at 5 GHz. For same volume fraction the nano-alumina composite has a relative permittivity of 3.52 and dielectric loss of 1.97×10^{-2} at 5 GHz. The high value of dielectric loss of nanocomposites is due to the presence of higher moisture content and large interface area of nanoparticles [34]. The connectivity among the filler particles and between the polymer and filler increases with filler loading. Porosity is also found to increase with increase in filler loading which is evident from the SEM images. The presence of porosity decreases the relative permittivity and increase the dielectric loss factor. However the effect of porosity is relatively smaller as compared to the effect of filler addition.

The following theoretical models are used to calculate the effective relative permittivity of SR-mAL composite at 5 GHz frequency.

Maxwell Garnet [35]

$$\frac{\varepsilon_{eff}-\varepsilon_m}{\varepsilon_{eff}+2\varepsilon_m}=f\,\frac{\varepsilon_i-\varepsilon_m}{\varepsilon_i+2\varepsilon_m} \tag{3}$$

Jayasundere–Smith equation [36]

$$\varepsilon_{eff}=\frac{\varepsilon_m(1-f)+\varepsilon_i f[\,3\varepsilon_m/(\varepsilon_i+2\varepsilon_m)]\;[1+(3f(\varepsilon_i-\varepsilon_m))/(\varepsilon_i+2\,\varepsilon_m)]}{(1-f)+f[3\varepsilon_m/(\varepsilon_i+2\varepsilon_m)][1+(3f(\varepsilon_i-\varepsilon_m))/(\varepsilon_i+2\varepsilon_m)]} \tag{4}$$

Lichtenecker equation [37]

$$\text{In}\;\varepsilon_{eff}=f\;\text{In}\;\varepsilon_i+(1-\text{f})\;\text{In}\;\varepsilon_m \tag{5}$$

Modified Lichtenecker equation [38]

$$\text{Log}\varepsilon_{eff}=\log\varepsilon_m+f\;(1-k)\log\left(\frac{\varepsilon_i}{\varepsilon_m}\right) \tag{6}$$

Effective Medium Theory (EMT) [39]

$$\varepsilon_{eff}=\left[1+\frac{f(\varepsilon_i-\varepsilon_m)}{\varepsilon_m+n(1-f)(\,\varepsilon_i-\varepsilon_m)}\right] \tag{7}$$

where ε_{eff}, ε_m and ε_i are relative permittivity of composite, matrix and filler, respectively and f is the volume fraction of the filler. Generally all the theoretical predictions are valid for low filler contents. At higher volume fractions the deviation is due to inhomogeneous dispersion of filler in matrix. Fig. 10 shows the comparison of experimental and theoretical values of relative permittivity of composite obtained from the above models. Many theoretical models suggest that the filler particle in a material should ideally be separated, non-interacting and roughly spherical [40]. Maxwell Garnet relations predict lower ε_r compared to the experimental data. This relation is suitable for very low volume fraction of ceramic particles. Reduction in depolarization of fillers and increase in relative permittivity, which are not accounted in this formula for higher filler loading [41]. Lichtenecker equation considers the composites are random

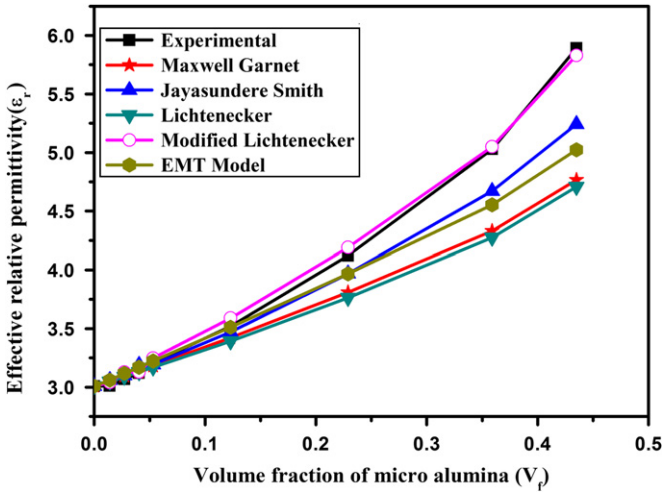

Fig. 10. Comparison of experimental and theoretical permittivity of SR-mAL composites at 5 GHz.

mixtures of spherical particles. From SEM micrograph it is clear that the particles are irregularly shaped and hence the deviation from Lichtenecker equation. Jayasundere–Smith equation is valid up to $0.1V_f$ of filler. This model considers composite as a bi-phase system of dielectric spheres (εf) dispersed in a continuous medium (ε_m) and is valid only when $\varepsilon_f > \varepsilon_m$ [23]. EMT model is valid only up to 0.1 volume fraction of filler. EMT model considers composite as an effective medium whose relative permittivity is the average relative permittivity of constituents. The complex effective permittivity will depend on the homogeneity of distribution of the filler, shape and size of filler; also interface between filler and matrix. EMT model includes a morphology factor '*n*' which gives the shape of the filler used in the polymer–ceramic composite. The shape factor n is determined from empirical calculations, which is found to be 0.15 for SR-mAL composites. However, the particle size should be small for better fitting with the theoretical predictions is the only restriction of EMT model. In the present case filler particles are not very small in size and hence show deviation from the experimental values. Among the models Modified Lichtenecker equation is in good agreement with the experimental values as shown in Fig. 10. In Modified Lichtenecker equation a fitting factor *k* is used which gives the interaction between the filler and matrix. Modified Lichtenecker model has been attempted to account the shape factor and distribution of the filler. Also the fitting factor is sensitive to polymer matrix and ceramics. The fitting factor for SR-mAL composite is -0.4774 which is in agreement with an earlier report [38].

Theoretical models for predicting the dielectric loss is relatively less and are more complicated. The following equations are used to model the loss tangent of composite.

General mixing model [42]

$$(\tan\boldsymbol{\delta}_c)^{\alpha} = \sum V_{fi}\,(\tan\boldsymbol{\delta}_i)^{\alpha} \tag{8}$$

tan δ_c and δ_i are the loss tangent of composite and *i*th material respectively,α is a constant, V_{fi} is the volume fraction of *i*th material. The value of constant α determines the mixing rule where $\alpha=-1$ (serial mixing) $\alpha=1$ (parallel mixing) and $\alpha=0$ gives logarithmic mixing rule.

The Bruggeman model [43]

$$\varepsilon'' = \frac{(\boldsymbol{\varepsilon}'_i-\boldsymbol{\varepsilon}')(\boldsymbol{\varepsilon}'_i+2\boldsymbol{\varepsilon}')\boldsymbol{\varepsilon}'}{(\boldsymbol{\varepsilon}_i-\boldsymbol{\varepsilon}'_m)(\varepsilon'_i+2\varepsilon')\varepsilon'_m}\varepsilon''_m + \frac{3(\boldsymbol{\varepsilon}'-\boldsymbol{\varepsilon}'_m)}{(\boldsymbol{\varepsilon}'-\boldsymbol{\varepsilon}'_m)(\boldsymbol{\varepsilon}'_i+2\boldsymbol{\varepsilon}')}\boldsymbol{\varepsilon}''_i \tag{9}$$

where $\boldsymbol{\varepsilon}'_i, \boldsymbol{\varepsilon}'_m, \boldsymbol{\varepsilon}', \boldsymbol{\varepsilon}''_i, \boldsymbol{\varepsilon}''_m$ and $\boldsymbol{\varepsilon}''$ are the real and imaginary part of the filler, matrix and the composite respectively. In the case of SR-mAL composite the major factor controlling the dielectric loss is the low tan δ value of the filler (4.3×10^{-5}) compared to the matrix (1.59×10^{-2}). But for nano-alumina, the loss is high due to the hydrophilic nature and large interaction volume of filler. Fig. 11 shows the comparison of dielectric loss of SR-mAL composite at 5 GHz with theoretical models. Parallel model gives a better fit to the experimentally observed values of tan δ. The parallel mixing rule shows a deviation at high volume fraction ($0.45V_f$) due to the agglomeration of filler. The Bruggeman model and Serial model failed to

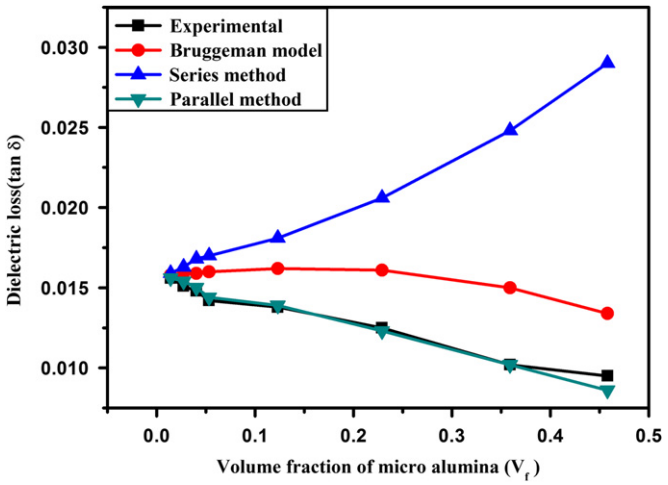

Fig. 11. Comparison of experimental and theoretical dielectric loss of SR-mAL composites at 5 GHz.

evaluate the dielectric loss of silicone rubber-micro-alumina composite. The dielectric loss of a composite depends on the intrinsic and extrinsic factors. The extrinsic factors such as defects, size and shape of fillers, micro-pores, etc. contributes to dielectric loss of composite. A new model satisfying both intrinsic and extrinsic factors need to be developed for better fitting with all volume fractions of filler [14,44].

The temperature dependence of relative permittivity ($\tau\varepsilon_r$) of both micro- and nano-alumina composites at 1 MHz are shown in Fig. 12(a) and (b), respectively. The temperature dependence of permittivity in polymers depends on two factors such as the glass transition temperature, *Tg*, and the frequency dependence of material [45]. It can be seen from the figures that the temperature variation of relative permittivity is relatively small in both the composites. Both SR-mAL and SR-nAL composites show a slight decrease in relative permittivity with increase in temperature for all the compositions. As the filler volume fraction increases from 0–0.45 the percentage deviation in ε_r decreases from about 9–5% for SR-mAL composites and for SR-nAL composites (0–$0.05V_f$) the deviation is about 9–6%. The large difference in CTE of the filler and matrix is responsible for the disturbance of aggregation of polar components and thus the decrease in relative permittivity with temperature [46,47]. Thus from the figures it can be concluded that the silicone rubber micro-alumina and silicone rubber nano-alumina composites show reasonably good temperature stability of relative permittivity.

3.6. Variation in coefficient of thermal expansion of the composites

Fig. 13 shows the variation of coefficient of thermal expansion of the SR-mAL and SR-nAL with filler volume fraction. A reduction in CTE was observed with increase in filler loading. CTE values of alumina filler and pure silicone

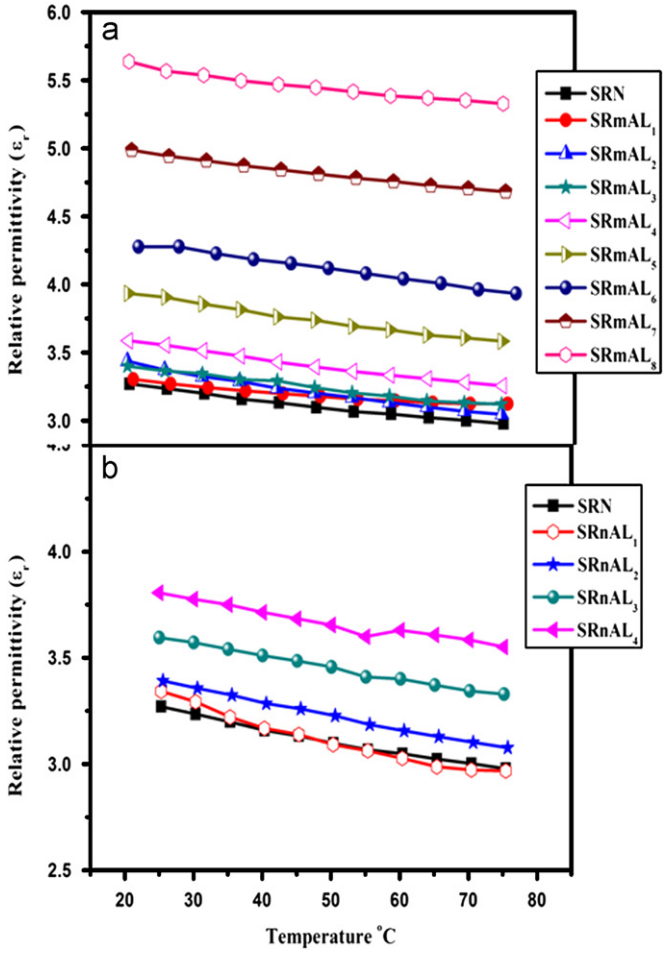

Fig. 12. Variation of relative permittivity with temperature for (a) SRmAL composites and (b) SRnAL composites at 1 MHz.

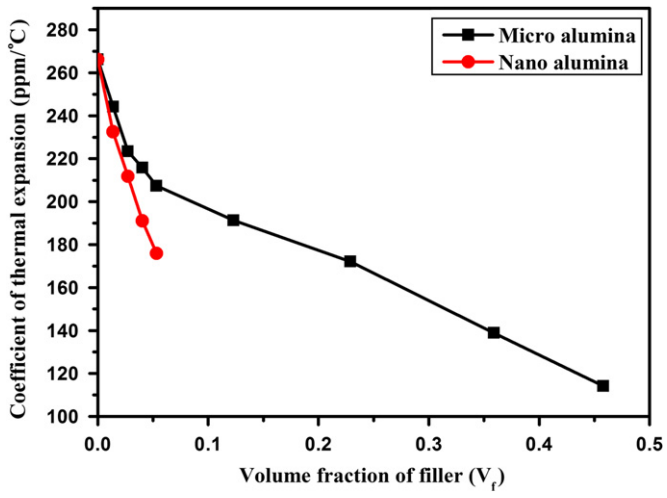

Fig. 13. Variation of CTE of (a) SR-mAL and (b) SR-nAL composites with ceramic content.

rubber are 7.2 ppm/°C and 266 ppm/°C, respectively. The CTE of 0.36 volume fraction of micro-alumina filled silicone rubber is 138 ppm/°C and 0.05 volume fraction of nano-alumina filled silicone rubber is 175 ppm/°C, compared to

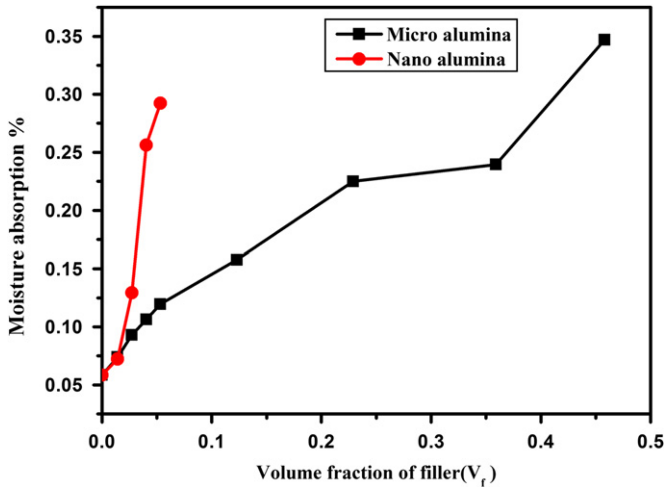

Fig. 14. Variation of moisture absorption of: (a) SR-mAL and (b) SR-nAL composites with filler loading.

unfilled silicone rubber (266 ppm/°C). The reason may be that there exist mechanical interaction between filler and matrix, which binds the matrix together preventing it from expanding as much as the unfilled matrix. In the case of nano-alumina the reduction in CTE is abrupt, because of the large surface area and the interaction volume of nano-alumina, which may block the thermal expansion of the matrix [48].

3.7. Variation in moisture absorption of the composites

Moisture absorption of the composite substrate material is very important since it adversely affects the dielectric properties of substrate for practical applications [34]. Variation in moisture absorption of alumina (micro and nano) loaded silicone rubber composite as a function of filler is given in Fig. 14. There is a large variation in moisture absorption of composites with micro- and nano-alumina. For microcomposite, the moisture absorption increases as filler loading increases because the porosity increases at high volume fractions. But in the case of nano-alumina, for a small volume fraction large increase in moisture absorption occurs which is due to the agglomeration of filler and hydrophilic nature of nanoparticles. This high moisture absorption may be a reason for large dielectric loss of nanocomposite.

4. Conclusions

Mechanically flexible and stretchable silicone rubber micro-alumina and silicone rubber nano-alumina composite were prepared in a kneading machine followed by hot pressing. The optimum temperature and duration for hot pressing were obtained from cross linking studies. The variation in dielectric properties at 1 MHz and 5 GHz, mechanical flexibility, coefficient of thermal expansion, temperature dependence of relative permittivity and moisture absorption of micro- and nano-alumina filled silicone

rubber matrix were investigated. The variation of relative permittivity with temperature showed that the SR-mAL and SR-nAL composites have good temperature stability of relative permittivity. Relative permittivity of both micro- and nano-alumina composite increased and loss tangent of micro-alumina decreased and that of nano-alumina increased with filler loading at 1 MHz and 5 GHz. For 0.05 volume fraction of micro-alumina composite, the relative permittivity is 3.21 and loss tangent is 1.42×10^{-2} at 5 GHz and for the same volume fraction of nano-alumina composite ε_r is 3.52 and tan δ is 1.97×10^{-2} at 5 GHz. Relative permittivity of 5.89 and tan δ of 9×10^{-3} is obtained for 0.45 volume fraction of micro-alumina composite at 5 GHz. The experimental values of relative permittivity and dielectric loss were compared with theoretical models. Among the different theoretical models Modified Lichtenecker and Parallel model are in good agreement with experimental values of ε_r and tan δ, respectively. The mechanical property is better for nano-alumina composites as compared to that of micro-alumina composite. The dielectric properties are good for micro-alumina composites for practical application. Coefficient of thermal expansion and moisture absorption were low for micro-alumina composite compared to nano-alumina composites. The micro-alumina filled silicone rubber composite is a good candidate for flexible microwave substrate application.

Acknowledgments

The authors are grateful to the Ministry of Human Resource and Development, New Delhi for the financial assistance. Dr. P. Prabhakar Rao and Mr. M. R. Chandran for SEM and Mr. Brahmakumar for tensile measurements.

References

[1] K. Jain, M. Klosner, M. Zemel, S. Raghunandan, Flexible electronics and displays: high-resolution, roll-to-roll, projection lithography and photo ablation processing technologies for high-throughput production, Proceedings of the IEEE 93 (2005) 1500–1510.

[2] J. Ryu, K.Y. Kim, J.J. Choi, B.D. Hahn, W.H. Yoon, B.K. Lee, D.S. Park, D.Y. Jeong, C. Park, Flexible dielectric $Bi_{1.5}Zn_{1.0}Nb_{1.5}O_7$ thin films on a Cu-polyimide foil, Journal of the American Ceramic Society 92 (2009) 524–527.

[3] W.S. Wong, A. Salleo, Flexible Electronics: Materials and Applications, Springer, USA, 2009.

[4] S.H. Park, H. Ko, C.P. Pan, A.P. Grigoropoulos, J.M.J. Pisano, E.S. Fréchet, J.H. Lee, Jeong, Nanoscale patterning and electronics on flexible substrate by direct nanoimprinting of metallic nanoparticles, Advanced Materials 20 (2008) 489–496.

[5] G. Subodh, V. Deepu, P. Mohanan, M.T. Sebastian, Polystyrene/$Sr_2Ce_2Ti_5O_{15}$ composites with low dielectric loss for microwave substrate applications, Polymer Engineering and Science 49 (2009) 1218–1224.

[6] D.L. Chung, Materials for Electronic Packaging, Butterworth-Heinemann publications, Boston, 1995.

[7] P.E. Garrou, I. Thurlik, in: Multichip Module Technology Handbook, Mc Graw-Hill, New York, 1998.

[8] M.B. Tian, Substrates for High Density Package Engineering, Beijing, Tsinghua University press, 2003.

[9] S. Rimdusit, H. Ishida, Development of new class of electronic packaging materials based on ternary systems of benzoxazine, epoxy, and phenolic resins, Polymer 41 (2000) 7941–7949.

[10] J.I. Hong, P. Winberg, L.S. Schadler, R.W. Siegel, Dielectric properties of zinc oxide/low density polyethylene nanocomposites, Materials Letters 59 (2004) 473–476.

[11] W.Y. Zhou, S.H. Qi, C.C. Tu, Novel heat-conductive composite silicone rubber, Journal of Applied Polymer Science 104 (2007) 2478–2483.

[12] S. Koulouridis, G. Kiziltas, Y. Zhou, D.J. Hansford, J.L. Volakis, Polymer–Ceramic composites for microwave applications: fabrication and performance assessment, IEEE Transactions on Microwave Theory and Techniques 54 (2006) 4202–4208.

[13] M.T. Sebastian, Dielectric Materials for Wireless Communication, Elsevier, Oxford, UK, 2008.

[14] M.T. Sebastian, H. Jantunan, Polymer–ceramic composites of 0–3 connectivity for circuits in electronics: a review, International Journal of Applied Ceramic Technology 7 (2010) 415–434.

[15] F. Qin, C. Brosseau, A review and analysis of microwave absorption in polymer composites filled with carbonaceous particles, Journal of Applied Physics 111 (2012) 061301(1)–061301(24).

[16] G. Gallone, F. Carpi, D. De Ross, G. Levitta, A. Marchetti, Dielectric constant enhancement in a silicone elastomer filled with lead magnesium niobate–lead titanate, Materials Science and Engineering C. 27 (2007) 110–116.

[17] S. Babu, K. Singh, A. Govindan, Dielectric properties of $CaCu_3Ti_4O_{12}$–silicone resin composites, Applied Physics A 107 (2012) 697–700.

[18] J.W. Liou, B.S. Chiou, Dielectric tunability of barium strontium titanate/silicone–rubber composite, Journal of Physics: Condensed Matter 10 (1998) 2773–2786.

[19] L.C. Sim, S.L. Ramanan, H. Ismail, Thermal characterization of Al_2O_3 and ZnO reinforced silicone rubber as thermal pads for heat dissipation purposes, Thermochimica Acta 430 (2005) 155–165.

[20] Q. Wang, Z.M. Xie, Highly thermally conductive room-temperature-vulcanized silicone rubber and silicone grease, Journal of Applied Polymer Science 89 (2003) 2397–2399.

[21] W.Y. Zhou, D. Yu, C. Wang, Q. An, S. Qi, Effect of filler size distribution on the mechanical and physical properties of alumina-filled silicone rubber, Polymer Engineering and Science 48 (2008) 1381–1388.

[22] T. Dhanesh, J. Chameswary, M.T. Sebastian, Mechanically flexible butyl rubber–$SrTiO_3$ composite dielectrics for microwave applications, International Journal of Applied Ceramic Technology 8 (2011) 1099–1107.

[23] J. Chameswary, T. Dhanesh, G. Subodh, H. Soumya, P. Jacob, M.T. Sebastian, Microwave dielectric properties of flexible butyl rubber–strontium cerium titanate composites, Journal of Applied Polymer Science 124 (2012) 3426–3433.

[24] L.E. Yahaya, K.O. Adebowale, A.R.R. Menon, S. Rugmini, B.I. Olu-Owolabi, J. Chameswary, Natural rubber/organoclay nanocomposites: Effect of filler dosage on the physicomechanical properties of vulcanizates, African Journal of Pure and Applied Chemistry 4 (2010) 198–205.

[25] M. Lovely, K.U. Joseph, J. Rani, Swelling behavior of isora/natural rubber composites in oils used in automobiles, Bulletin of Material Science 29 (2006) 91–99.

[26] E.A. Rashid, K. Ariffin, H. Akil, Mechanical and thermal properties of polymer composites for electronic packaging application, Journal of Reinforced Plastics and Composites 27 (2008) 1573–1584.

[27] N. Mohamad, A. Muchtar, M.J. Ghazali, D.H. Mohd, C.H. Azhari, The effect of filler on epoxidised natural rubber-alumina nanoparticles composites, European Journal of Scientific Research 24 (2008) 538–547.

[28] W. Zhou, S. Qi, H.Z. Zhao, N.L. Liu, Thermally conductive silicone rubber reinforced with boron nitride particle, Polymer Composites 28 (2007) 23–28.

[29] L.E. Nielsen, R.F. Landel, in: Mechanical Properties of Polymers and Composites, 2nd ed., Marcel Dekker Inc, New York, 1994.

[30] Y. Zhou, H. Wang, L. Wang, K. Yu, Z. Lin, L. He, Y. Bai, Fabrication and characterization of aluminum nitride polymer matrix composites with high thermal conductivity and low dielectric constant for electronic packaging, Materials Science and Engineering B 177 (2012) 892–896.
[31] D.H. Kuo, C.C. Chang, T.Y. Su, W.K. Wang, B.Y. Lin, Dielectric properties of three ceramic/epoxy composites, Materials Chemistry and Physics 85 (2004) 201–206.
[32] T. Hu, J. Juuti, H. Jantunen, T. Vilkman, Dielectric properties of BST/polymer composite, Journal of the European Ceramic Society 27 (2007) 3997–4001.
[33] S.K. Battacharya, R.R. Tummela, Next generation integral passives: materials, processes, and integration of resistors and capacitors on PWB substrates, Journal of Materials Science: Materials in Electronics 11 (2000) 253–268.
[34] K.P. Murali, S. Rajesh, O. Prakash, A.R. Kulkarni, R. Rathesh, Preparation and properties of silica filled PTFE flexible laminates for microwave circuit applications, Composites Part A 40 (2009) 1179–1185.
[35] P.S. Anjana, V. Deepu, S. Uma, P. Mohanan, J. Philip, M.T. Sebastian, Dielectric, thermal, and mechanical properties of CeO_2-filled HDPE composites for microwave substrate applications, Journal of Polymer Science Part B: Polymer Physics 48 (2010) 998–1008.
[36] N. Jayasundere, B.V.J. Smith, Dielectric constant for binary piezoelectric 0–3 composites, Applied Physics 73 (1993) 2462–2466.
[37] H. Sihvola, Self-consistency aspects of dielectric mixing theories, IEEE Transactions on Geoscience and Remote Sensing 27 (1989) 403–415.
[38] T. Sherin, V. Deepu, S. Uma, P. Mohanan, P. Jacob, M.T. Sebastian, Preparation, characterization and properties of $Sm_2Si_2O_7$ loaded polymer composites for microelectronic applications, Materials Science and Engineering B 163 (2009) 67–75.
[39] Y. Rao, J. Qu, T. Marinis, C.P. Wong, A precise numerical prediction of effective dielectric constant for polymer-ceramic composite based on effective-medium theory, IEEE Transactions on Components and Packaging Technologies 23 (2000) 680–683.
[40] D. Stroud, Percolation effects and sum rules in the optical properties of composites, Physical Review B 19 (1979) 1783–1791.
[41] S. Rajesh, K.P. Murali, K.V. Rajani, R. Ratheesh, $SrTiO_3$-Filled Ptfe composite laminates for microwave substrate applications, International Journal of Applied Ceramic Technology 6 (2009) 553–561.
[42] R. Abraham, R. Guo, S. Bhalla, Modeling Permittivity and Tangent Loss in Dielectric Materials Using Finite Element Method and Monte Carlo Simulation, Ferroelectrics 315 (2005) 1–15.
[43] X.X. Wang, K.H. Lam, X.G. Tang, H.L.W. Chan, Dielectric characteristics and polarization response of lead-free ferroelectric (Bi0.5Na0.5)0.94Ba0.06TiO3–P(VDF-TrFE) 0–3 composites, Solid State Communications 130 (2004) 695–699.
[44] G. Subodh, V. Deepu, P. Mohanan, M.T. Sebastian, Dielectric response of high permittivity polymer ceramic composite with low loss tangent, Applied Physics Letters 95 (2009) 062903-1–062903-3.
[45] B.J.P. Adohi, C. Brosseau, Dielectric relaxation in particle-filled polymer: Influence of the filler particles and thermal treatments, Journal of Applied Physics 105 (2009) 054108-1–054108-8.
[46] T. Sherin, V.N. Deepu, P. Mohanan, M.T. Sebastian, Effect of filler content on the dielectric properties of PTFE/$ZnAl_2O_4$–TiO_2 composites, Journal of the American Ceramic Society 91 (2008) 1971–1975.
[47] G.M. Tsangaris, G.C. Psarras, The dielectric response of a polymeric three-component composite, Journal of Materials Science 34 (1999) 2151–2157.
[48] S. Kemaloglu, G. Ozkoc, A. Aytac, Properties of thermally conductive micro and nano size boron nitride reinforced silicon rubber composites, Thermochimica Acta 499 (2010) 40–47.